

# INVESTIGATIONS OF CONVECTIVE CLOUDS WITH ICE-PHASE PROCESS

**Masaki Katsumata, Hiroshi Uyeda and Taro Shinoda**

*Division of Earth and Planetary Sciences,  
Graduate School of Science, Hokkaido University, Sapporo 060-0810 JAPAN*

The ice-phase process plays important role on the cloud system, by affecting the vertical redistribution process of energy and water, especially in the middle and upper troposphere for the tropical / extratropical area. For example, Uyeda et al. (1995) showed that the result of the TOGA/COARE observation. The paper suggests that the part above freezing level is important in the mechanism of tropical cloud cluster: convection reinforced above the freezing level by freezing of raindrops, or the independent updraft above the freezing level existed in the stratiform region. These suggest that the more investigation about the ice-phase process is necessary to recognize the structure of mesoscale convective systems. The behavior of cloud water and cloud ice is essential in the investigation. On the observational approach, however, only few devices detect cloud water and cloud ice. Among them, only the mobile / scanning microwave radiometer can obtain the horizontal structure,

Snow clouds are suitable object to obtain the data only for the ice-clouds, as shown by Katsumata et al. (1998). To verify the effect of simple but detailed horizontal and vertical structure of the clouds to the microwave radiation, the observation by the airborne microwave radiometer (AMR) of NASDA was carried out for snow clouds in the winter of 1995/1996 and 1996/1997, in the Sea of Japan. Because snow clouds are low in the cloud top (< 5km), they are easy to compare with ground-based data. On the AMR observation, the X-band Doppler radar, from National Research Institute of Earth Sciences and Disaster Prevention (NIED) of Japan, observed same object simultaneously with the AMR.

Figures 2 and 3 show the result. In Fig.2, the vertical cross section of radar reflectivity shows that the precipitation core was located in the upper part of the convective cell. Around the core, the Doppler velocity field shows convergence in the lower part, while divergence in the upper part. These indicate that the cell was in the developing stage. In correspond to the cell, the  $T_B$  at 89GHz vertically polarized channel ( $T_{B89V}$ ) shows minimum value (thick solid line) on the precipitation core. In the cell, cloud water rich part was also detected by both  $T_B$  and polarization ratio ( $P$ ,  $P = T_{BH} / T_{BV}$ ) on 89- and 36-GHz channels, which show maximum value (thick broken line). On the other hand, no  $T_B / P$  maximum were found on another cell in dissipating stage, as shown in Fig.3. These result shows that the microwave radiometer is effective to reveal horizontal structure, of convective clouds, including location of the updraft, and to estimate vertical structure. However, the microwave radiometer data are affected by the vertical profile of the hydrometers, not only the vertically integrated amount, as shown in Fig.4. The vertical distribution of cloud water and cloud ice is effective to quantitative estimation of the vertical / three-dimensional distribution of the hydrometers. The information must support our knowledge about the snow clouds and mesoscale convective systems with ice-phase process.

On the other hand, numerical simulation provide the distribution of the cloud water and cloud ice separately in fine spatial / temporal resolution. The example is shown in Figure 5: the result of numerical simulation of weak tropical cloud cluster, using two-dimensional cloud-resolution model (Yoshizaki and Ogura, 1988) with ice-phase parameterization by Murakami (1990). In the figure, the mixing ratio of the cloud water was higher than that of rain / snow / graupel. It suggests that the cloud water and cloud ice is indispensable factor to understand the structure of the convective system. However, the amount of cloud ice in the result is smaller than expected. In addition, only few observational data can validate the result, especially about the ice-phase parameterization. The cloud radar must also contribute to improve the numerical model. The simulated reflectivity for cloud radar (Fig. 5d) suggests that minimum detectable sensitivity of -30dBZ ensure to use the data from cloud radar for the investigation of convective clouds.

< References >

Katsumata, M., H. Uyeda and K. Kikuchi, 1998: Characteristics of a cloud band off the west coast of Hokkaido Island as determined from AVHRR/NOAA, SSM/I and Radar Data. *J. Meteor. Soc. Japan*, **76**, in press.

Liu, G. and J. A. Curry, 1993: Determination of characteristic features of cloud liquid water from satellite microwave measurements. *J. Geophys. Res.*, **98**, 5069--5092.

Murakami, M., 1990: Numerical modeling of dynamical and microphysical evolution of an isolated convective cloud — The 19 July 1981 CCOPE cloud —. *J. Meteor. Soc. Japan*, **68**, 107-128.

Uyeda, H, M. Katsumata, et al., 1995: Doppler radar observation of the structure and characteristics of tropical clouds during the TOGA-COARE IOP in Manus, Papua New Guinea. — Outline of the observation —. *J. Meteor. Soc. Japan*, **73**, 415-425.

Yoshizaki, M. and Y. Ogura, 1988: Two- and three-dimensional modeling studies of the Big Thompson storm. *J. Atmos. Sci.*, **45**, 3700-3722.

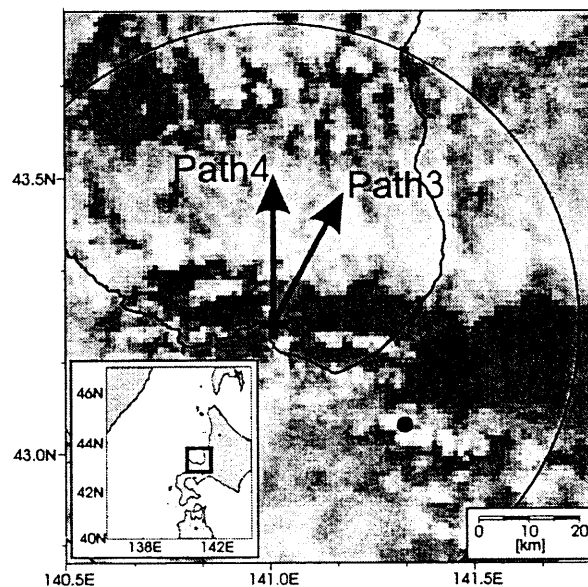


Fig. 1: AVHRR/NOAA infrared image at 0354GMT on February 16, 1996. The circle and cross show the observation range and location of NIED radar. The dot shows the location of the aerological observation site of Sapporo. The arrows show the direction of two paths of AMR observation, Path 3 and Path 4.

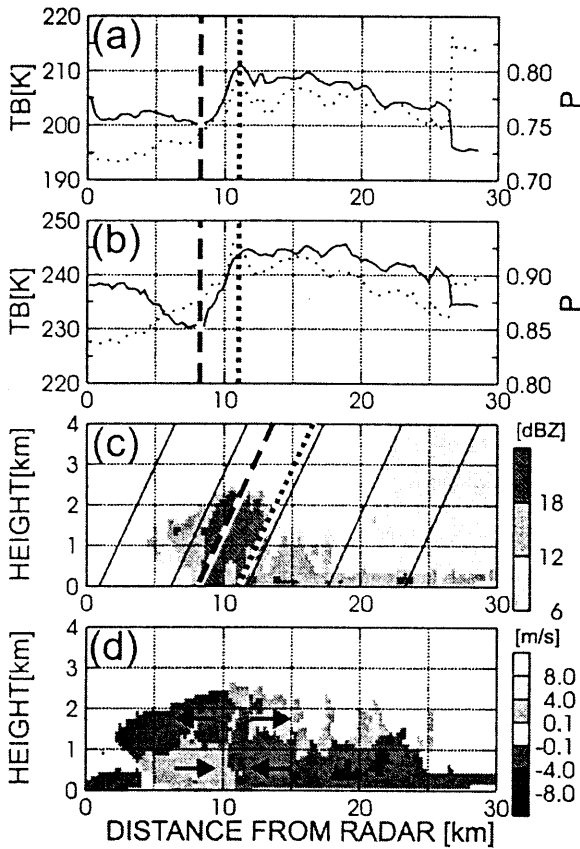


Fig. 2: Example of the result of simultaneous observation by AMR and Doppler radar, for Path 4 in Fig. 1. (a)  $T_{B36v}$  (thin solid line) and  $P_{36}$  (thin dotted line), (b)  $T_{B89v}$  (thin solid line) and  $P_{89}$  (thin dotted line), (c) radar reflectivity, and (d) Doppler velocity. AMR data, (a) and (b), are plotted on the point where the antenna horn pointed at surface level, and ray paths every 1 minute are shown as solid lines in (c). See article for thick broken and thick dotted lines.

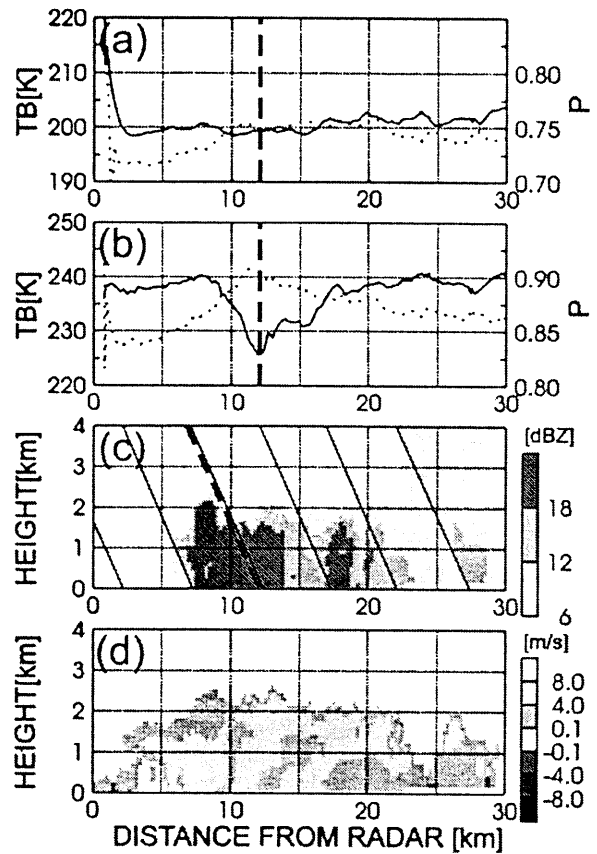


Fig. 3: Same as Fig. 2, but for another cross section, Path3 in Fig. 1.

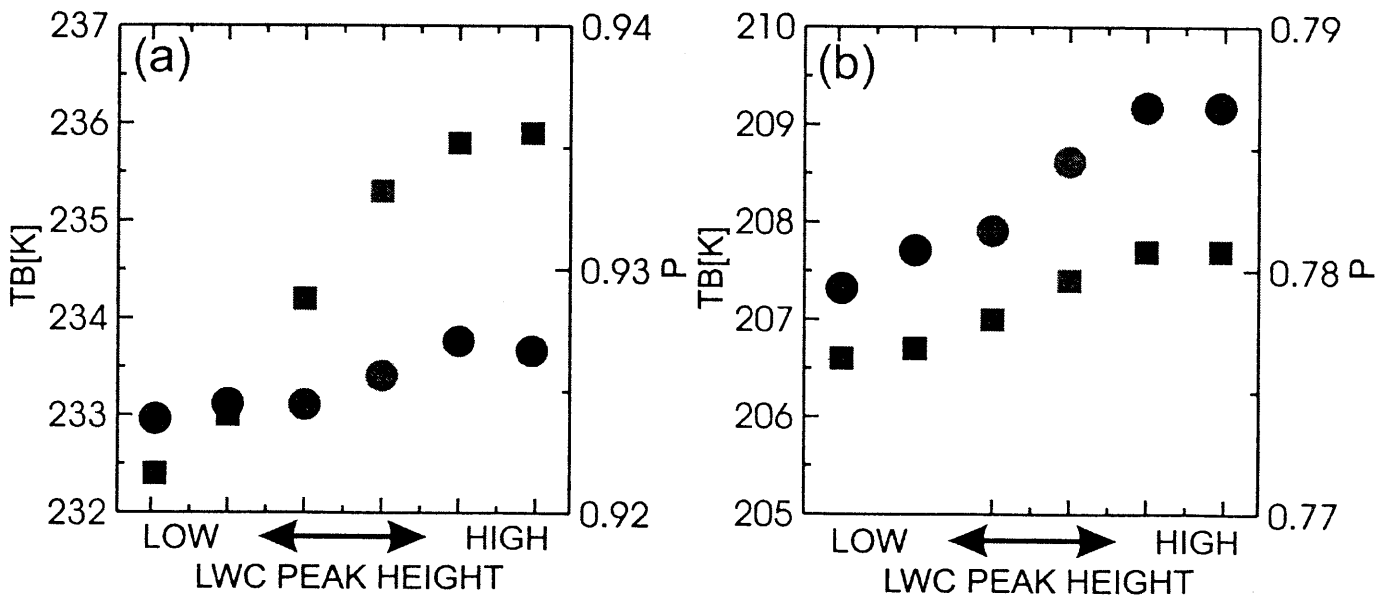


Fig. 4: Results of the radiative transfer simulation for six different vertical distributions of liquid water but for same liquid water path. (The other factors are also fixed). Brightness temperature (dot) and polarization ratio (square) on (a) 89-GHz channels and (b) 36-GHz channels are plotted.

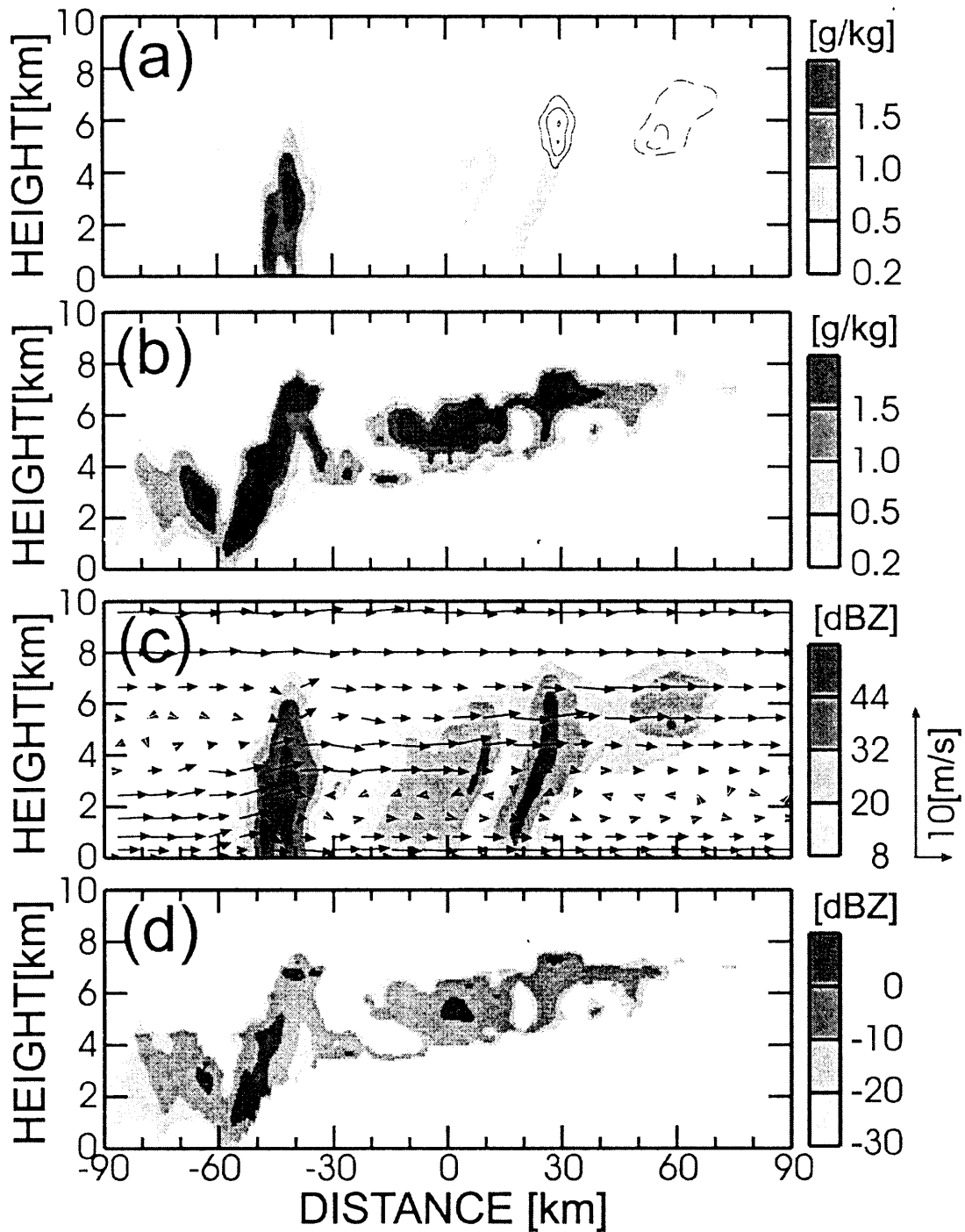


Fig.5: Example of the result of numerical simulation of a tropical cloud cluster: (a) mixing ratio of rain (shade), graupel (solid contour) and snow (broken contour), (b) mixing ratio of cloud water (shade) and cloud ice (solid contour), (c) estimated radar reflectivity for rain, graupel and snow, and (d) estimated radar reflectivity for cloud water and cloud ice. Rayleigh approximation is adopted to estimate radar reflectivity in (c) and (d).